Superpressure Balloons as Isentropic/Isopycnic Tracers

RALPH D. REYNOLDS

Atmospheric Sciences Laboratory, U. S. Army Electronics Command, White Sands Missile Range, N. M. 88002

(Manuscript received 1 November 1971, in revised form 27 November 1972)

ABSTRACT

Synchronous radar, temperature and pressure data of suitable quality, gathered from three balloon flights of the Mountain Wave Project, were analyzed in detail to show the relationships between balloon-depicted waves and isentropic and isopycnic waves. Results show that in wave conditions, superpressure balloons: 1) follow the undulations of density surfaces but overestimate crests and troughs of waves by an average error of 6%; and 2) follow isentropic surfaces, but underestimate true wave crests by an average error of 5%, and true wave troughs by errors averaging 30%.

1. Introduction

Use of superpressure balloons in the study of mountain waves at White Sands Missile Range from 1963–69 stimulated speculation as to how unerringly the flow of such a balloon will coincide with the flow of a free air parcel. In their computer program simulations of balloons floating through a sinusoidal wave (Fig. 1), Hirsch and Booker (1966) calculated that a 0.17 m^3 pillow superpressure balloon would underestimate the amplitude and would indicate the position of maxima and minima of vertical velocities far upstream of the actual; they determined that in the first wave downwind of a barrier, a balloon would show the wave amplitude 15% lower than actual.

Three Mountain Wave Project balloon flights (Lamberth *et al.*, 1965), having synchronous radar, temperature and pressure data of suitable quality, were analyzed in detail to show the relationship between the balloon-depicted wave and the isentropic and isopycnic waves. The balloons used in this study were spherical, with diameters of 1.9 and 2.15 m.

2. Discussion

A superpressure balloon is a balloon of nonextensible fabric, designed to float, with an internal pressure always greater than the ambient atmosphere. The balloons used in this study had superpressures of 10 mb. Greenfield and Davis (1963) determined that the ultimate floating altitude of a balloon occurs at the point where atmospheric density is described by

$$\rho_f = M_L/[V(1-M_a/M_g T_b/T_f)], \quad (1)$$

where:

ρ_f	density at floating altitude
M_L	gross mass of the balloon and payload
V	volume of the balloon
M_a/M_g	density ratio of air to gas at equal temperature
T_b/T_f	temperature ratio of the minimum balloon temperature during ascent to the temperature at balloon float altitude.

As is shown in Eq. (1), a superpressure balloon is an isopycnic vehicle, and such a balloon should therefore be expected to follow an isopycnic surface except where the forces on the balloon impell it to move with or near the free air flow.

The vertical equation of motion of a balloon, used by Hanna and Hoecker (1971) is

$$M_b\frac{\partial w_b}{\partial t} = M_a\frac{\partial w_a}{\partial t} + \tfrac{1}{2}M_a\left(\frac{\partial w_a}{\partial t} - \frac{\partial w_b}{\partial t}\right) - M_b g\left(\frac{\rho_b-\rho_a}{\rho_b}\right) - \rho_a A\frac{C_d}{2}(w_b-w_a)|w_b-w_a|, \quad (2)$$

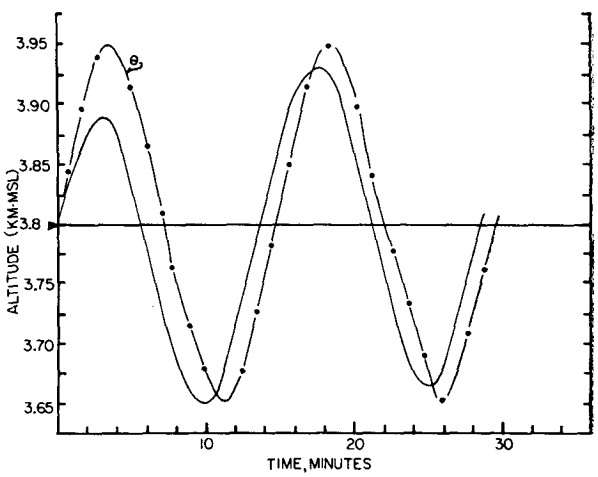

FIG. 1. From their computer program, Hirsch and Booker showed that a 0.17 m^3 pillow superpressure balloon would underestimate the amplitude and would indicate the position of maxima and minima of vertical velocities too far upstream; the solid line is the path of their theoretical balloon and the dot-dash line is their calculated isentropic surface.

where:

M_b total mass of the balloon and payload (gm)
M_a mass of the air displaced by balloon system (gm)
w_a vertical speed of the air (cm sec^{-1})
w_b vertical speed of the balloon (cm sec^{-1})
g acceleration of gravity (cm sec^{-2})
ρ_a density of air (gm cm^{-3})
ρ_b density of the balloon system (gm cm^{-3})
A cross-sectional area presented to the vertical air stream by the balloon (cm^2)
C_d drag coefficient

As shown by Eq. (2), the net force on the balloon equals the dynamic buoyancy force, plus the acceleration drag force, minus both the static buoyancy force and the drag force. For example, at the inflection point of a mountain wave in a downdraft where $w_b=-480$ cm sec^{-1}, $w_a=-500$ cm sec^{-1}, $\rho_a=8\times10^{-4}$ gm cm^{-3}, $\rho_b=6\times10^{-4}$ gm cm^{-3}, $C_d=1$, the net force on a two meter diameter balloon is:

Net force $=-3.8\times10^4$ dyn
Dynamic buoyancy force $=-1.65\times10^6$ dyn
Acceleration drag force $=-3.3\times10^4$ dyn
Static buoyancy force $=-1.5\times10^6$ dyn
Drag force $=5\times10^3$ dyn

We see that, at the inflection of a wave, the two buoyancy forces are two orders of magnitude greater than the greatest of the drag forces. At the trough of a wave with $w_b=0$ and $w_a=-1$ cm sec^{-1}, the net force $=1.5\times10^6$ dyn, where the static buoyancy force is three orders of magnitude greater than any other force.

The superpressure balloons were released upwind of White Sands Missile Range and tracked simultaneously by FPS-16 radars and GMD radiosonde receivers. Radar digital data were recorded at one point per second and smoothed over 30-sec intervals. Data from flights 135 and 265 were reduced under contract with the Meteorology Department, UCLA. The potential temperature and density data for flight 265 were computed by using the continuous temperature and pressure from an AMT-15 radiosonde that had been modified with our continuous pressure device (Glass *et al.*, 1968). Flight 265 was reduced at White Sands; continuous pressure sensor data and continuous temperature data were available on this flight. Baroswitch pressure and continuous temperature from an AMT-15 clock-switched radiosonde were used to compute isentropic and density data for flight 135. Pressure data were computed from a combination of baroswitch low references, radar heights, and the hydrostatic equation. The radar-tracked balloon curves in Figs. 2–7 were plotted for each 30 sec and to the nearest meter.

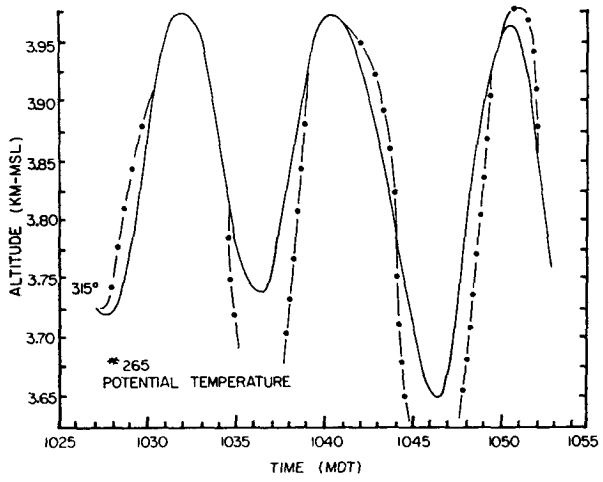

FIG. 2. The 30-sec averaged height of the balloon tracked by FPS-16 radars (solid curve), and the isentropic surface, calculated from continuous temperature and continuous pressure from balloon instrumentation (dot-dash line). The theoretical float altitude for the balloon in an undisturbed atmosphere was 3.80 km. In the first radar-tracked balloon trough at 1036 MDT, the air parcel is estimated to have sunk 65 m below the balloon. In the second wave, the balloon undershot the isentropic trough by 130 m.

3. Data analysis

For balloon flights 135 and 265, potential temperatures recorded each 30 sec along the entire track of the balloon were added, and a mean potential temperature for the entire flight was obtained; any deviations from this mean isentropic surface were converted into height differences, determined by assumed gradients, above or below the radar track of the balloon. Isentropic gradients in moderate waves usually range from 50–130 m per potential temperature degree, as has been shown by the Boulder Mountain Wave studies (Kuettner and Lilly, 1968). When a gradient of 65 m per potential temperature degree is assumed, substantial agreement with Hirsch's and Booker's analysis is obtained.

For each of the above-mentioned flights, density values recorded each 30 sec along the entire track of the balloon were added, and a mean density for the entire flight was obtained; any deviations from this isopycnic surface were converted into height differences, determined by assumed gradients, above or below the radar track of the balloon. Isopycnic gradients assumed in this study are 10 gm m^{-3} per 100 m at 3.8 km and 8 gm m^{-3} per 100 m at 5.8 km. These potential temperature and density gradients agree with others reported for numerous computer-reduced rawinsonde observations, conducted at White Sands during mountain wave conditions while our studies were in progress.

In Fig. 2, the phase and amplitude of the isentropic wave is shown to be in agreement with the radar-tracked balloon wave until near the nadir of the first balloon-tracked trough at 1036 MDT; here, the air parcel is estimated to have sunk 65 m below the balloon depicted wave, but then it reestablished coincidence with the balloon at the second crest. The balloon underestimates the bottom of the second isentropic trough by ~130 m, crosses the isentropic surface near the third crest, then underestimates the third isentropic

crest by ~18 m (5%). It is seen that the balloon, at the bottom of the troughs, deviates from the maximum wave height of the balloon tracked wave by 19–38%.

Maximum vertical velocities of mountain waves occur at the inflection points of the waves. At this point on the upslope of the first wave, the balloon wave slope is steeper than the isentropic wave slope, and the balloon inflection point lags behind the isentropic inflection point. On the downslope of the first crest, the slopes of the balloon and isentropic wave are equal at 3.835 km and occur together. On the upslope of the second crest, the balloon inflection point is ahead or upstream of the isentropic wave's inflection point, and the balloon slope is not as steep as the isentropic wave slope. This means that the balloon does not indicate as high a vertical velocity as the free parcel. On the downslope of the second wave, the balloon's inflection point is upstream of the isentropic surface's inflection point, and the balloon slope is less than the isentropic slope. The maximum vertical velocity of the balloon is upstream of the isentropic wave on the upslope of the third wave and is not as great as that experienced by the free air parcels. In concurrence with the Hirsch and Booker theory, the overall phase of these balloon-tracked waves is advanced slightly upstream of the isentropic waves. The theoretical floating altitude of the balloon in undisturbed air is 3.8 km.

Low reference pressure contact, radar height, and the hydrostatic relationship were used to calculate pressure measurements on flight 135. A comparison of the isentropic wave and balloon wave for flight 135 is shown in Fig. 3. Again, the balloon wave is upstream of the isentropic wave. On the upslope of the first crest, the slope of the isentropic wave is greater than that of the balloon wave. On the downslope of the first wave,

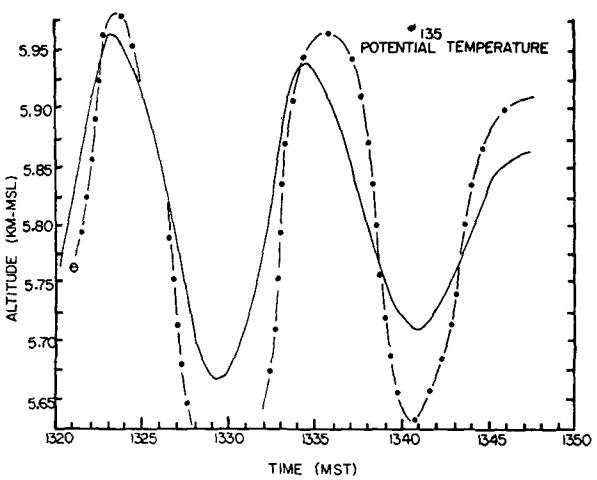

FIG. 3. The isentropic surface (θ) for flight 135 computed by using the low reference contact, the FPS-16 radar height, and the hydrostatic relationship. In this case, the balloon underestimates the first trough by 130 m and the second trough by 65 m; it also underestimates all three wave crests. The balloon-tracked wave phase is slightly ahead of the isentropic wave. This situation agrees with Hirsch and Booker's computations.

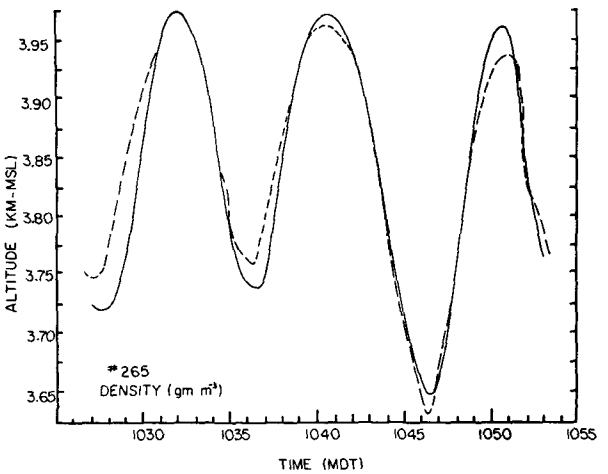

FIG. 4. The balloon (solid curve) lags behind the isopycnic surface in the first ridge but slight differences are evident in both the subsequent ridges and troughs. The phase in the third crest is slightly disparate; the balloon-depicted wave is ahead of the computed isopycnic wave.

the slope of the isentropic wave is steeper than the balloon wave. The balloon in the first trough is estimated to undershoot the isentropic trough by 130 m. The upslope and downslope of the isentropic wave in the second wave is steeper than that of the balloon-tracked wave. Balloon inflection points in the second wave are upstream of isentropic inflection points, and the balloon is estimated to undershoot the second trough by 65 meters. Again, it underestimates the height of each isentropic crest by 20, 25 and 45 m, respectively, or by errors of 6–14% of the maximum balloon-tracked wave height. In this case, we see probable errors of the balloon-tracked wave underestimating the isentropic wave troughs by 20–40%. The theoretical float altitude of this balloon in undisturbed flow is 5.8 km.

The isopycnic/balloon tracked relationship is shown in Fig. 4. It is seen that in the first two troughs at 1027 and 1036 MDT respectively, the balloon is 30 and 20 m lower than the isopycnic wave. This is an error of 6–9% of the maximum measured wave height of the balloon-tracked wave. The balloon underestimates the third trough by 15 m.

At the first crest, the balloon-tracked wave agrees with the isopycnic wave, but at the second and third crests, it overshoots the isopycnic wave by 10 and 25 m, producing errors of less than 8%. Phase agreement is good in the first and second crests but the balloon wave is ahead of the isopycnic wave in the third crest. The average error at crests and troughs is 6%.

In Fig. 5, the isopycnic, balloon-phase relationship is good except for the second crest where the balloon wave is upstream of the isopycnic wave. Errors in the first, second and third crests are 20%, 3% and 2%. The balloons overshot the two troughs by 8 and 10%. In this case, the maximum error of the balloon-tracked

wave to the computed isopycnic wave is 20% and the average error 9%.

Fig. 6 shows an interesting example of a balloon passing through very strong wave action and turbulence. The balloon's erratic behavior, dissimilar to what we had seen before, caused us to think that the balloon had burst or sprung a leak. But when potential temperatures along the balloon track were plotted for each time the potential temperature changes by 2C, it was discovered that an expansive area of downdraft, situated behind the mountain, was responsible for these vagaries. At the left side of the figure, to the windward of the mountain peak, rapid, short wavelengths, more indicative of turbulence, occur at an altitude where a nearby radiosonde reported dry adiabatic lapse rates within 1 hr of this flight. The wave leeward of the peaks carried the balloon into such a declivity that it was lost to the radar for 13 min, then the balloon rose slightly at 1410 MST, only to be forced lower and lower in other strong downdrafts. In fact, the balloon was ultimately forced 100 m below the lowest altitude shown here. The higher value potential temperatures show the excursions of air from higher altitudes.

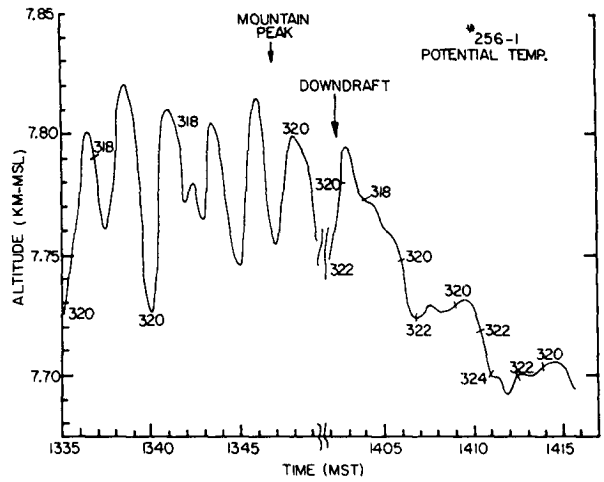

FIG. 6. Path of an FPS-16 radar-tracked superpressure balloon that was caught in turbulent high-frequency waves prior to reaching the mountain peak in a dry adiabatic layer. The downdraft was so severe leeward of the mountain that the balloon was lost to radar for 13 min. The potential temperature is plotted where it changed by 2C. The extreme downdrafts from 1404–1416 were accompanied by a severe dust wall over the eastern half of White Sands Missile Range. The balloon was ultimately forced 100 m below the lowest altitude shown here.

4. Conclusions

If the isentropic surfaces, predicated as they are on assumed gradients, are reasonable, these cases demonstrate two conclusions: first, that superpressure balloon-depicted waves indicate the maxima and minima of vertical velocities upwind of their true position; second, that these velocities are of not as great a magnitude as free air vertical velocities. The balloon-depicted wave crests are from 0 to 14% lower than the calculated free air wave crests, which yields an average error of 5%, while the balloon-depicted troughs are usually 20–40% less than the computed free air troughs, or in error by 30%.

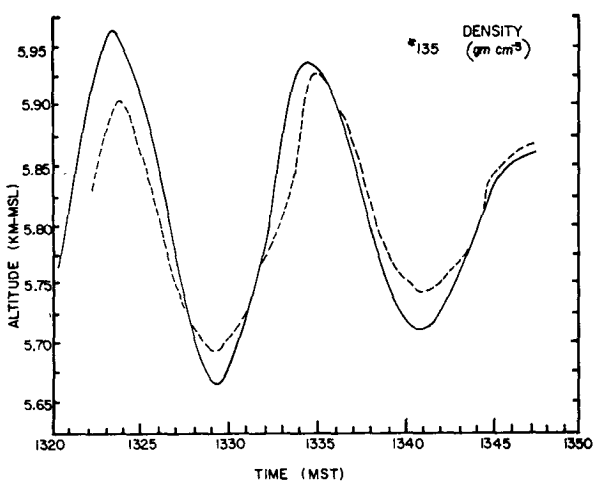

FIG. 5. The balloon (solid curve) is 60 m higher than the computed isopycnic surface in the first ridge, but, other than a slight phase lead in the second ridge, represents the isopycnic surface with overshoot errors of 35 m or less in the bottoms of the troughs.

The calculated isentropic waves are considered to be accurate approximations of the real air flow for flights 265 and 135. Balloons forced above their equilibrium float altitude responded to air flow on the upslope, but as they approached the wave crests where the vertical velocity of the air lessened, the weight of the balloon and the negative lift caused them to fall even before the air motion became downward. Likewise, when the balloons were forced below their equilibrium float altitude, balloon buoyancy counteracted drag forces of the downward moving air and caused the balloons to underestimate the actual mountain wave troughs.

As shown in Eq. (1), superpressure balloons are isopycnic vehicles; results demonstrate that, under wave conditions, superpressure ballons overestimate isopycnic crests and troughs by an average of 6%. The largest single error (20%) can not be explained.

While the author realizes that this size sample is not statistically significant, I feel that these balloon flight cases are indicative of true balloon-isopycnic relationships.

Acknowledgments. The constructive criticism of Dr. Morton G. Wurtele, Department of Meteorology, UCLA, in the preparation of this paper is appreciated.

REFERENCES

Glass, Roy I., Ralph D. Reynolds and Roy L. Lamberth, 1968: A high-resolution continuous pressure sensor modification for radiosondes. *J. Appl. Meteor.*, **7**, 141–144.

Greenfield, S. M., and M. H. Davis, 1963: The physics of balloons and their feasibility as exploration vehicles on Mars. The Rand Corp., Santa Monica, Calif., 43–50.

Hanna, Steven R., and Walter H. Hoecker, 1971: The response of constant-density balloons to sinusoidal variations of vertical wind speeds. *J. Appl. Meteor.*, **10**, 601–604.

Hirsch, John H., and D. Ray Booker, 1966: Response of superpressure balloons to vertical air motions. *J. Appl. Meteor.*, **5**, 226–227.

Lamberth, Roy I., Ralph D. Reynolds and M. G. Wurtele, 1965: Mountain lee waves at White Sands Missile Range. *Bull. Amer. Meteor. Soc.*, **46**, 634–636.

Kuettner, J. P., and D. K. Lilly, 1968: Lee waves in the Colorado Rockies. *Weatherwise*, **21**, 180–197.